UCLA

UCLA Electronic Theses and Dissertations

Title

Satellite cell proliferation and activation are activated by HIIT exercise and dampened by the klotho transgene through the reduction of canonical Wnt signaling.

Permalink

https://escholarship.org/uc/item/7049g152

Author

Barrington, Alice Rose

Publication Date

2021

Peer reviewed|Thesis/dissertation

eScholarship.org Powered by the California Digital Library
University of California

UNIVERSITY OF CALIFORNIA

Los Angeles

Satellite cell proliferation and activation are activated by HIIT exercise and dampened by the *klotho* transgene through the reduction of canonical Wnt signaling.

A thesis submitted in partial satisfaction

of the requirements for the degree of Master of Science

in Physiological Science

by

Alice Rose Barrington

2021

ABSTRACT OF THE THESIS

Satellite cell proliferation and activation are activated by HIIT exercise and dampened by the klotho transgene through the reduction of canonical Wnt signaling

by

Alice Rose Barrington

Master of Science in Physiological Science

University of California, Los Angeles, 2021

Professor James G. Tidball, Chair

The regenerative capacity of skeletal muscle requires muscle stem cells called satellite cells. Muscle injuries activate satellite cells to proliferate and then they either differentiate and fuse to existing muscle fibers, or they return to their quiescent state. The necessity of satellite cell proliferation and fusion for hypertrophic growth caused by increased muscle loading is contested (Egner et al. 2017). Although some studies demonstrate that satellite cells are required for hypertrophic growth after synergist ablation, other investigations show that hypertrophy can occur in muscles that are satellite-cell-deficient (Englund et al. 2011). We analyzed a high intensity interval training (HIIT) protocol that was designed to induce muscle growth (Goh et. al 2019) to determine whether growth in that model was accompanied by expansion of satellite cell numbers. Although satellite cell proliferation and activation were both increased following HIIT, hypertrophy did not occur. This suggests that satellite cell proliferation and activation are not

coupled to muscle hypertrophy in HIIT or that the magnitude of expansion of satellite cell numbers was insufficient to increase muscle growth. We then tested whether further expansion of satellite cell numbers in HIIT would produce hypertrophy by subjecting mice that express a transgene encoding Klotho to HIIT because our previous work has shown that Klotho can increase satellite cell proliferation *in vitro* and their numbers *in vivo*. Contrary to our expectation, the Klotho transgene attenuated the increases in satellite cell proliferation and activation that occurred in wild-type mice. We then explored the mechanism through which Klotho could attenuate satellite cell proliferation caused by exercise. Because previous investigators showed that signaling through the Wnt-β-catenin pathway increases satellite cell activation in exercised muscle (Fujumaki et al. 2014) and because Klotho can inhibit Wnt signaling in other cell types, we assayed whether expression of the Klotho transgene reduced Wnt-signaling in satellite cells in exercised muscle. Our findings showed that wild-type, exercised mice experienced increased β-catenin signaling in satellite cells after exercise, but the Klotho transgene diminished that effect. These findings suggest that Klotho may attenuate satellite cell activation in exercised muscle by inhibiting the canonical Wnt signaling pathway.

The thesis of Alice Rose Barrington is approved.

Scott H. Chandler

Victor R. Edgerton

Eisuke Ochi

James G. Tidball, Committee Chair

University of California, Los Angeles

2021

TABLE OF CONTENTS

LIST OF FIGURES

ACKNOWLEDGEMENTS

I would like to thank my thesis advisor, Dr. James Tidball for his support and encouragement throughout my graduate education. I am very grateful as well to my committee members for their guidance. I would especially like to thank Dr. Eisuke Ochi, whose mentorship, advice, and help was of great value.

Thank you to my friends and family for providing an excellent support system during my graduate education, and helping me to reach my goals.

Introduction

Skeletal muscle adapts to environmental stresses such as disease, injury, or exercise. The adaptation of skeletal muscle to external stimuli is crucial for its maintenance and growth. Exercise can promote muscle growth both directly and indirectly. Exercise-induced mechanical stress can directly promote muscle growth through intracellular signalling cascades. For example, mammalian target of rapamycin complex 1 (mTORC1) signaling causes muscle protein synthesis in response to mechanical stimuli (Wackerhage et al., 2019; Bamman et al., 2018). Exercise can also promote muscle growth through indirect influences. The mechanical stress to muscle induced by exercise results in stretching of a population of myogenic stem cells, called satellite cells (Tatsumi et al., 2001). *In vitro* experiments have demonstrated the activation of satellite cells following stretching, initiating a cascade of events that has been demonstrated to occur with hypertrophy (Goh et al., 2019).

Satellite cells are located between the basal lamina and the cell membrane of muscle fibers and exist in either a quiescent or activated state (Dhawan & Rando, 2005). During myogenesis, and in response to muscle damage, the myogenic process begins with the activation and proliferation of satellite cells (Charge & Rudnicki, 2004). Activated, proliferative satellite cells can either differentiate to form new myofibers or return to their quiescent state to maintain their population (Dhawan & Rando, 2005). Throughout each stage of myogenesis, satellite cells express different transcription factors (Dhawan & Rando, 2005). Pax7 is a basic helix-loop-helix transcription factor expressed in both quiescent and activated satellite cells. Activated satellite cells express the transcription factors MyoD and Myf5 which initiate transcription of muscle-specific genes necessary for early differentiation (Charge & Rudnicki, 2004). Proliferative MyoD+ and Myf5+ cells, called myoblasts, further differentiate and begin to express myogenin

at which time satellite cell fusion can occur (Charge & Rudnicki). There is a large body of work demonstrating that exercise induces increases in satellite cell number, and also induces hypertrophy (Shefer et al., 2013; Goh et al., 2019).

Although exercise induced muscle hypertrophy is often concurrent with increases in satellite cell number, the requirement of satellite cells for muscle fiber growth is debated (Shefer et al., 2013; Brooks et al., 1985; Goh et al., 2019). The requirement of satellite cells activation and fusion for hypertrophy is frequently attributed to the need of additional myonuclei to meet the transcriptional demand of a larger cytoplasm on the existing myonuclei (Murach et al., 2018). Multiple studies have demonstrated that following exercise or injury, muscle growth and regeneration does not occur without satellite cell involvement (Lepper et al., 2011). Muscle fiber hypertrophy that caused by life-long voluntary exercise is attenuated in mice with depleted satellite cell numbers (Englund et al., 2020). Further supporting this, a more stringent hypertrophy model using synergist ablation caused hypertrophy in untreated mice, but not in satellite cell deficient mice (Egner et al., 2016). Interestingly, other studies have contested these findings (McCarthy et al., 2011). In a similar synergist ablation model, satellite cell deficient mice were able to mount a robust hypertrophic response to mechanical overload (McCarthy et al., 2011). These conflicting findings leave the question of whether satellite cells are necessary for hypertrophic growth following exercise.

Exercise can induce the release of soluble factors that have the potential to affect hypertrophy. For example, Klotho is a soluble factor that is released at elevated levels during exercise (Ramez et al., 2019). First identified as an anti-aging protein, Klotho has the ability to increase satellite cell numbers and muscle fiber size in diseased and injured muscle (Wehling-Henricks et al., 2016; Welc et al., 2019). Expression of a *klotho* transgene in the mdx mouse

model of Duchenne muscular dystrophy significantly increased the satellite cell pool and improved longevity and function of skeletal muscle (Wehling-Henricks et al., 2016). Increased Klotho levels can also improve regeneration of muscle in response to muscle injury (Welc et al., 2019). Following injury, *klotho*-transgenic mice contained more Pax7+ cells and had increased fiber cross-sectional area compared to wildtype mice suggesting that Klotho affects muscle growth potentially by increasing satellite cell number (Welc et al., 2019). *Klotho* transgene expression also induced an increase in numbers of MyoD+ cells after acute injury, indicating that it affects the onset of satellite cell differentiation (Welc et al., 2019).

Klotho's effect on diseased and injured muscle may be mediated by its effects on Wnt signaling. Canonical Wnt signaling is characterized by the binding of extracellular Wnt proteins to their receptor, resulting in an intracellular signaling cascade that prevents the phosphorylation and subsequent degradation of β-catenin (Fujimaki et al., 2014). Canonical Wnt signaling can alter the expression of muscle specific genes in muscle stem cells (Fujimaki et al., 2014). Klotho reduces Wnt signaling *in vitro* and *in vivo*. Recombinant Klotho protein inhibits Wnt signalling in aged muscle stem cells (Ahrens et al., 2018). Increased expression of the *klotho* transgene reduced expression of Wnt target genes in injured muscles *in vivo*, demonstrated by reductions in numbers of satellite cells that express β-catenin (Welc et al., 2019). Klotho antagonism of Wnt signalling accelerated early muscle regeneration and repair following injury (Welc et al., 2019).

Wnt signaling can affect myogenesis by influencing both satellite cell proliferation and muscle differentiation. In muscle stem cells, β-catenin can form activator complexes that bind to DNA and increase the expression of genes that are necessary for muscle fiber regeneration and differentiation (Fujimaki et al., 2014). During skeletal muscle regeneration, Wnt signaling induces satellite cell proliferation (Fujumaki et al., 2014) In addition, canonical Wnt signaling is

up regulated in muscle during exercise, resulting in the increased expression of Myf5 and MyoD which are expressed in activated satellite cells (Fujimaki et al., 2014). These findings indicate the critical role of Wnt signaling in myogenesis and growth following exercise.

In this study, we test the hypothesis that expression of the *klotho* transgene will alter satellite cell proliferation and activation following exercise, potentially mediated through Wnt signaling. Using a high intensity interval training (HIIT) protocol that has been previously used to induce hypertrophy, we also aim to further investigate whether hypertrophic growth following exercise is coupled to increases in satellite cell number (Goh et al., 2019).

Materials and Methods

Animals

All animal experimentation complied with guidelines established by the UCLA Animal Research Committee. C57BL/6J mice were purchased from the Jackson Laboratory and bred and housed in a pathogen-free vivarium. Mice carrying the *klotho* transgene were crossed onto the C57BL/6 background for a minimum of six generations (Welc et al. 2019). 10 wildtype and 9 *klotho* transgenic mice were sacrificed at five to six months old by inhalation of isoflurane. The right tibialis anterior muscle was weighed, flash frozen, and stored in liquid-nitrogen-cooled isopentane for histological analysis. The left tibialis anterior muscle was frozen in liquid nitrogen for qPCR analysis.

High-intensity interval training (HIIT)

Our 8-week, high-intensity training (HIIT) protocol was modeled on a previously reported HIIT protocol designed to increase the amount of work performed each week (Goh et al 2019). HIIT sessions were completed on an Exer-6M Treadmill from Columbus Instruments. Prior to HIIT, mice were acclimated to the treadmill during week 0 by running three times at a speed of 8m/min for 15 minutes with no incline (Figure 1A). Mice were subjected to 3 sessions of HIIT per week for 8 weeks. For the first 3 weeks of HIIT, there was a weekly 5° increase in the angle of inclination of the treadmill from 10° at week 1 up to 20° at week 3. From weeks 3 to 8, the treadmill incline was maintained at 20°. Each session consisted of a 5-minute warm-up at 8

m/min, followed by eight exercise intervals at the prescribed speed and angle of inclination for 3-5 minutes, with 1-minute breaks at 8 m/min between intervals. During weeks 1-4, treadmill speed increased over the 8 sessions from 15-16 m/min. During week 5, 6, 7 and 8, treadmill speed increased from 15-17 m/min, 15-18 m/min, 15-19 m/min, and 15-20 m/min, respectively. Mice that did not stay on the treadmill were shocked by an electric stimulus from the shock grid beneath the treadmill at a current of 4 mA and a repetition rate of 5 Hz. Mice that did not quickly resume running after landing on the shock grid were manually guided back on the treadmill. Mice that did not resume running frequently after manual assistance were excluded from the study.

Immunohistochemistry

Cross sectional area:

Cross sections of 10-μm thickness were taken from the mid-belly of tibialis anterior muscles frozen in isopentane. Sections were incubated in hematoxylin for 10 minutes, and subsequently rinsed with distilled H_2O.

Stained sections were imaged using a digital imaging system (Bioquant). The area and minimum Feret diameter of 500 randomly-selected fibers per cross section was measured using ImageJ. Small, average, and large fibers were determined by calculating 3 standard deviations from the mean cross-sectional area (CSA). Small fibers were classified as less than 3 standard deviations from the mean cross-sectional area, and large fibers were classified as more than 3 standard deviations from the mean.

Pax7+ cells:

Sections were dried for 30 minutes and fixed in 4% paraformaldehyde for 10 minutes. The sections were submerged in antigen retrieval buffer (10 mM sodium citrate, 0.05% Tween 20, pH 6.0) for 40 minutes at 95°C. Sections were then incubated in 0.3% hydrogen peroxide in phosphate buffered saline (PBS) for 10 minutes to quench endogenous peroxidase activity. A mouse-on-mouse immunohistochemistry kit (M.O.M kit, Vector Laboratories, Burlingame, CA, USA) was used to treat the sections with blocking buffer for 60 minutes, followed by immunolabeling with affinity purified mouse anti-Pax7 (1:500) overnight at 4°C. The sections were then labeled with biotin conjugated anti-mouse IgG (1:250) for 30 minutes and incubated with ABC reagent from the M.O.M kit. Staining was visualized with the peroxidase substrate 3-amino-9-ethylcarbazole (AEC; Vector Laboratories), yielding a red reaction product.

Pax7+ cells were quantified in sections by observations through an Olympus BH50 microscope (Center Valley, PA, USA) using a 40x objective lens, with the sections overlaid with a 10 x 10 eyepiece micrometer grid. The number of cells per volume was determined by counting the number of grid intercepts overlying tissue in the field and multiplying this value by the section thickness (10 μm). The numbers of satellite cells were counted and expressed as the number of cells per unit volume in the section. The numbers of satellite cells were also expressed as the number of cells per one hundred fibers.

MyoD+ cells:

Sections were dried for 30 minutes and fixed in cold acetone for 10 minutes, then air dried for 10 minutes. After immersion in PBS sections were incubated in 0.3% hydrogen peroxide in PBS for

10 minutes to quench endogenous peroxidase activity, washed in PBS and then incubated in M.O.M kit blocking buffer for 60 minutes. The sectioned tissues were subsequently washed with PBS and incubated in goat anti-mouse Fab fragment (1:10) for one hour. Then, after washing with PBS, sections were incubated overnight at 4°C in mouse anti-MyoD (BD Pharmingen; Cat #554130 1:50) diluted in protein dilutent from the M.O.M kit. Following primary antibody incubation, sections were washed in PBS and incubated in M.O.M kit secondary anti-mouse IgG (1:200) for 30 minutes. The sections were then incubated with ABC reagent from the M.O.M kit. Staining was visualized with the peroxidase substrate 3-amino-9-ethylcarbazole (AEC; Vector Laboratories), yielding a red reaction product.

MyoD+ cells were quantified in sections following the same procedure for counting Pax7+ cells as described above.

Developmental myosin heavy chain (dMHC):

Sections were stained following the same procedure as described for MyoD+ cell counts, but instead using mouse anti-dMHC (Novacastra; NCL-MHCd Lot# 6067485 1:100).

dMHC+ regenerating fibers were quantified in sections by observations through an Olympus BH50 microscope as described above. The numbers of regenerating fibers were counted and expressed as the number of cells per section area.

Dystrophin/hematoxylin myonuclei:

Sections were fixed and blocked following the same procedure as the anti-MyoD protocol. Sections were incubated overnight at 4°C in mouse anti-dystrophin (Novacastra; NCL-DYS2

Lot# 6067485 1:30) diluted in protein dilute from the M.O.M kit. Following primary antibody incubation, sections were washed in PBS and incubated in M.O.M kit secondary anti-mouse IgG (1:200) for 30 minutes. The sections were then incubated with ABC reagent from the M.O.M kit. After incubating the sections in tap water for 1.5 minutes, they were incubated in hematoxylin for 3 minutes, and subsequently rinsed with tap water. Dystrophin staining was visualized with the peroxidase substrate 3-amino-9-ethylcarbazole (AEC; Vector Laboratories), yielding a red reaction product.

Myonuclei were quantified in sections by observations through an Olympus BH50 microscope as described above. The number of cells per 500 fibers was determined by counting the number of hematoxylin-stained nuclei residing within the dystrophin border of 500 total fibers.

Immunofluorescence:

Pax7/β-catenin double labeling:

The double labeling protocol was similar to the anti-Pax7 method described above. Mouse anti-Pax7 (SCBT 1:50) and rabbit anti- β-catenin (CST 1:1500) were applied to sections. After overnight incubation, sections were incubated with anti-mouse Dylight594 (1:100) and anti-mouse Dylight 488 (1:100) for one hour. After a final wash with PBS, the sections were mounted with ProLong Gold Antifade Mount with DAPI and cover slipped. Numbers of β-catenin positive satellite cells were expressed as a proportion of total satellite cells per section.

MHC IIa and IIb double labeling:

Cross sections were fixed in acetone as described previously. Sections were immersed in PBS and then immersed in solution consisting of 3% bovine serum albumin (BSA), 0.2% gelatin, and 0.05% Tween-20, (blocking buffer), for 30 minutes. The sectioned tissues were then washed with PBS and incubated overnight at 4°C in mouse anti-MHCIIa IgG and anti-MHCIIb IgM (Developmental Studies Hybridoma Bank SC-71, BF-F3, neat). Following the primary antibody incubation, the sections were washed in PBS. The sections were incubated in their respective secondary antibodies, anti-mouse IgG1 Alexa Fluor 488 (1:500), and anti-mouse IgM Alexa Fluor 555. Sections were cover slipped and mounted as described in the double labeling procedure above. The proportion of type IIa, IIb, and IIx fibers was quantified in sections by observations through an Olympus BH2 microscope (Center Valley, PA, USA) using a 40x objective lens. Total numbers of total fibers, type IIa and type IIb fibers were counted. Numbers of type IIx fibers were determined by subtracting type IIa and type IIb fibers from the total.

Cell culture:

Frozen BF-F3 and SC-71 cells were purchased from Developmental Studies Hybridoma Bank (DSHB). Cells were thawed for 2 minutes in a 37°C water bath, transferred to a centrifuge tube and spun down at 170 x g for 5 minutes. After withdrawing the supernatant, the cell pellet was resuspended in growth medium and transferred to a T75 flask. Cells were placed in an incubator at 37° C with 5.0% CO_2. After cell growth, cells were split into more T75 flasks. For cell freezing, cells that were in log phase growth and at a density of approximately 5 x 10^5 were spun at 170 x g for 5 minutes. Cells were resuspended in freezing medium, (growth medium with 6% DMSO), and aliquoted into cryovials for freezing. For supernatant preparation, cells were maintained in the incubator at an approximate density of 5 x 10^5 to which serum-free medium

was added daily. Cells were allowed to enter stationary and eventually death phase over approximately 14 days. The culture was spun at 670 x g for 10 minutes, and the supernatant was collected. After adding 6 mls of 1M Tris-HCl pH 7.5 and sodium azide to each 200 mls of supernatant, aliquots were stored at -20°C.

RNA isolation:

RNA was isolated from 50 mg of frozen tibialis anterior muscles following homogenization in Trizol (Life Technologies). to pellet insoluble material, homogenized samples were centrifuged at 12,000 g for 10 minutes at 4°C. The supernatant containing the RNA was incubated at room temperature for 5 minutes. Chloroform (20% of the original Trizol volume) was added to each sample, and each sample was vortexed for 15 seconds. After the samples were incubated at room temperature for 3 minutes, the samples were centrifuged at 12,000 g for 20 minutes at 4°C to fractionate them into three distinct layers: a clear phase (aqueous, RNA phase), interphase (protein) and organic phase (protein and DNA: phenol). The aqueous layer containing the RNA was transferred into a new tube, and approximately 50% of the original Trizol volume of isopropyl alcohol was added. The samples were subsequently mixed by inversion and then incubated at room temperature for 10 minutes. The samples were next centrifuged at 12,000 g for 20 minutes at 4°C, resulting in a white RNA pellet. The pellet was resuspended in 1.2 ml of 75% ethanol and centrifuged at 7,500 g for 5 minutes at 4°C. The supernatant was removed, and the pellet was air dried on ice and then resuspended in RNase-free water. RNA samples were purified with RNeasy Mini Kit (Qiagen). RNA concentrations were determined using a Beckman DV730 spectrophotometer (Beckman Coulter) at wavelengths of 260 nm and 280 nm. All

samples had a 260/280 ratio greater than 2.0; RNA quality was assessed via 1.2% agarose gel electrophoresis. RNA isolation experiments were performed by Professor Eisuke Ochi.

Quantitative real-time polymerase chain reaction (qPCR):

To generate cDNA, a master-mix consisting of Oligo(dT)12-18 primer (Invitrogen) and 10 mM dNTPs was added to samples containing either 1 or 2 μg of RNA. The samples were subsequently incubated at 65°C for five minutes. A reverse transcriptase master-mix consisting of SuperScript™ II RT (Invitrogen), First-Strand Buffer (Invitrogen), 0.1 M dithiothreitol (Invitrogen), and nuclease-free H2O was added to each sample. The samples were then incubated at 42°C for 50 minutes, then at 70°C for 50 minutes to heat inactivate the enzyme. The final cDNA sample was diluted 1:1 in sterile water and stored at -20°C. qPCR analysis was performed using 96-well plates. Each well contained 2 μl of cDNA and 23 μl of a master mix (autoclaved water, SYBR® Green Supermix (Bio-Rad) and the corresponding forward and reverse primers for the gene of interest (Table 1). Reference genes used were Srp14 and Rpl13a for all tissue and cell samples. Experiments were performed on a Quantstudio 5 Real-Time PCR System (Thermo Fisher). qPCR experiments were performed by Professor Eisuke Ochi.

Statistical Analysis:

All statistical analyses were performed using unpaired Student t-tests or two-way ANOVA with differences considered significant at $p < 0.05$. All graphs display mean ± standard error of the mean (SEM).

Gene	**Forward**	**Reverse**
klotho	GTCTCGGGAACCACCAAAAG	CTATGCCACTCGAAACCGTC

Table 1. Primer Sequence

Results

High Intensity Interval Training (HIIT) does not affect *klotho* expression in wild-type or *klotho* transgenic mice.

To investigate the effects of HIIT on mouse skeletal muscle, a HIIT protocol was developed based on previous studies (Goh et al 2019). 6-month wild-type and *klotho* transgenic mice underwent the eight-week training protocol in which the intensity and speed were increased over time (Figure 1A). *Klotho* relative expression was increased in *klotho* transgenic mice compared to wild-type, as measured by qPCR (Figure 1B, Table 1). qPCR experiments were performed by Professor Eisuke Ochi. However, the HIIT protocol did not result in changes in the expression of *klotho* in the wild-type or *klotho* transgenic mice (Figure 1B)

Klotho transgene expression attenuates the increase in numbers of total satellite cells and activated satellite cells caused by HIIT.

Previous studies demonstrated that following acute skeletal muscle injury, elevated expression of *klotho* increases the numbers of Pax7+ and MyoD+ cells *in vivo* (Welc et al 2019). *In vitro*, the application of Klotho along with its cofactor FGF23 to myoblasts increases their proliferation (Wehling-Henricks et al 2016). These findings led us to investigate the whether the *klotho* transgene would increase satellite cell numbers and activation following exercise in skeletal muscle.

In wild-type mice, HIIT increased Pax7+ cells (Figure 2A, B). Interestingly, in the presence of the *klotho* transgene, the number of Pax7+ cells were not significantly increased following HIIT (Figure 2A, B). A similar pattern was observed in numbers of MyoD+ cells, where HIIT induced an increase in activated satellite cells in wild-type mice that was attenuated by the *klotho* transgene (Figure 2D, E). These data suggest that the *klotho* transgene attenuates changes in satellite cells that occur following HIIT.

Klotho transgene expression in mice experiencing HIIT increases numbers of myonuclei and the number of dMHC+ fibers.

The reductions in Pax7+ and MyoD+ cell numbers following HIIT in *klotho* transgenic muscle could be a result of Klotho-mediated reductions in myoblast proliferation. However, these reductions could also result from a more rapid progression of muscle cell differentiation and fusion. Perhaps a Klotho-mediated increase in speed of differentiation and fusion could explain a decrease in satellite cell number and activation compared to wild-type at the point of sacrifice immediately following HIIT. To investigate this possibility, we quantified numbers of myonuclei and newly formed dMHC+ fibers as indicators of fusion and differentiation.

Numbers of myonuclei were increased in *klotho* transgenic compared to wild-type mice both with and without exercise (Figure 3A). *Klotho* transgenic mice also exhibited an increase in dMHC+ fibers compared to wild-type mice (Figure 3C). The observed increases in numbers of myonuclei and dMHC+ fibers in *klotho* transgenic mice that underwent HIIT suggest that the *klotho* transgene increases the speed of muscle cell differentiation and fusion during the 8 week

protocol. Increases in satellite cell number and activation following HIIT that are attenuated by the *klotho* transgene could represent slower muscle cell differentiation in wild-type mice (Figure 2A, D).

Klotho transgene expression prevents activation of the canonical Wnt pathway that results from HIIT.

Considering the attenuation of Pax7+ and MyoD+ cell increases in *klotho* transgenic mice after HIIT, we next investigated a potential pathway through which Klotho could act. A previous study demonstrated that following acute muscle injuries, reductions in MyoD+ cells caused by the *klotho* transgene coincided with reductions in canonical Wnt signaling (Welc et al 2019). To determine whether the Klotho transgene similarly prevents activation of the canonical Wnt pathway following HIIT, we measured numbers of satellite cells positive for the active form of β-catenin.

HIIT induced an increase in β-catenin+ satellite cells in wild-type mice, suggesting an increase in canonical Wnt signaling (Figure 4A). However, the *klotho* transgene attenuated the increase in numbers of β-catenin+ satellite cells following exercise (Figure 4A). Similar to the effects of Klotho after acute muscle injury, the *klotho* transgene results in a reduction in MyoD+ cells that coincides with a reduction in the activation of canonical Wnt signaling following HIIT (Figure 2D, 4A).

Klotho transgene expression increases the proportion of small diameter fibers in non-exercised and exercised muscles.

Following acute muscle injury, and in *mdx* mice, elevated expression of *klotho* increases fiber growth (Welc et al 2019). Previous study also demonstrated an increase in fiber mass and area following exercise, causing us to ask whether the *klotho* transgene caused fiber growth in exercised skeletal muscle in our HIIT model (Goh et al 2019).

Fiber CSA and diameter were measured to assay for hypertrophic effects of HIIT exercise and *klotho* transgene expression. No changes in average CSA or diameter were caused by HIIT or the presence of the *klotho* transgene, indicating that neither HIIT or HIIT with *klotho* over-expression induces hypertrophy in our model (Fig. 5A-F). We next assayed whether HIIT or *klotho* transgene expression affected the distribution of fiber sizes by binning fibers into small, average or large CSA groups (Fig. 5G, H). Although HIIT did not affect the proportion of fibers that were present in the three groups in either the wild-type or transgenic mice, expression of the transgene caused an increase in the proportion of fibers that were present in the small CSA and large CSA groups, compared to the frequency distribution in wild-type mice (Fig. 5G, H).

HIIT increases the proportion of type IIa fibers in wild-type but not *klotho* transgenic muscles.

We next tested whether the increased proportion of small CSA fibers in *klotho* transgenic muscles reflected an increase in the proportion of small diameter, oxidative fibers. A previous study demonstrated that life-long voluntary exercise causes a shift from a glycolytic to oxidative

fiber type (Englund et al 2020). To determine whether HIIT alone or in combination with the *klotho* transgene results in a fiber type shift, we quantified fiber type distribution. Although HIIT produced a significant increase in type IIa fibers in wild-type muscles, suggesting a shift towards more oxidative muscle fibers (Figure 6M), HIIT did not increase the proportion of type IIa fibers in *klotho* transgenic mice (Figure 6M). In addition, expression of the *klotho* transgene prevented an HIIT-induced increase in the proportion of type IIa fibers (Figure 6M). HIIT did not induce changes in either type IIb or type IIx in either wild-type or transgenic mice (Figure 6 N, O).

Discussion

In this study we demonstrate that satellite cell proliferation and activation are increased by HIIT exercise but are dampened by the *klotho* transgene through the reduction of canonical Wnt signaling. These findings further elucidate the effects of Klotho on Wnt signaling, and how these alterations to Wnt signaling impact myogenesis following exercise. Although our HIIT model induced increases in Pax7+ and MyoD+ cells in wild-type mice, it did not have the same effect in *klotho* transgenic mice. These data could indicate that *klotho* attenuates the increases in myogenesis following HIIT. However, increased numbers of myonuclei and dMHC+ cells in *klotho* transgenic exercised mice indicate that the *klotho* might instead be accelerating myogenesis.

Our data demonstrating Klotho's attenuation of the increases of Pax7+ and MyoD+ cell number following HIIT suggests an inhibitory effect of Klotho on myogenesis. Our findings showed that the satellite cells of wild-type muscle exhibited increased Wnt signaling following exercise that coincided with increases in Pax7+ and MyoD+ cell numbers. This supports previous investigations into satellite cell changes following voluntary wheel running, where canonical Wnt signaling via β-catenin modulated the chromatin structure of the MyoD gene, and increased numbers of MyoD+ cells (Fujumaki et al., 2014). While HIIT increased Wnt signaling and accelerated myogenesis in wildtype mice, the addition of the *klotho* transgene attenuated these effects. Together, these findings indicate that the Klotho's attenuation of myogenesis after exercise may be mediated by inhibition of canonical Wnt signaling. A previous study of acute muscle injury in which expression of the *klotho* transgene reduced Wnt signaling in Pax7+ cells, corresponding to reduced numbers of MyoD+ cells (Welc et al., 2019) supports our findings in the current investigation. The reduction of Wnt signaling induced by Klotho observed in our

study is also consistent with other findings that demonstrate that Klotho can bind to and inhibit extracellular Wnt proteins (Liu et al., 2007).

Seemingly in contrast, the *klotho* transgene reduced MyoD+ cell numbers, suggesting inhibited myogenesis, but the *klotho* transgenic increased the number of myonuclei in exercised mice, suggesting accelerated myogenesis. This increase in myonuclear accretion perhaps indicates that reductions in numbers of Pax7+ and MyoD+ cells in transgenic mice could be attributed to increased differentiation and fusion of myogenic cells, rather than inhibition of their activation and differentiation. Similarly, the observed increase in dMHC+ fibers in exercised *klotho* transgenic compared to exercised wildtype mice further supports the idea that the *klotho* transgene is accelerating myogenesis. Our data therefore indicate that activated Wnt/ β-catenin signaling after exercise keeps satellite cells in a proliferative or activated state in wild-type mice, the attenuation of which by the *klotho* but the transgene then accelerates the differentiation and fusion of those cells. In our study, sample collection occurred on the last day of eight weeks of exercise. At this time point, exercised skeletal muscle of wild-type mice appears to be beginning the myogenic process with satellite cell proliferation and activation, while *klotho* transgenic exercised muscle progressed to myogenic cell fusion to new and existing fibers.

Although HIIT induced changes in myogenesis represented by increases in satellite cell number and activation in klotho transgenic mice, these changes surprisingly did not coincide with a hypertrophic response of the muscle in wild-type or *klotho* transgenic muscle. Our study further investigates the link between satellite cells and hypertrophy. We demonstrate that increases in satellite cell number because of HIIT are not correlated with an increase in hypertrophy at the time point that the muscles were assayed. This suggests that changes in satellite cell number and fiber growth are uncoupled processes. Whether satellite cells are

required for hypertrophic growth of muscle following exercise is contested. A study reported that hypertrophy does not occur in satellite cell deficient mice following muscle overload through synergist ablation (Egner et al. 2016). However, other work demonstrated hypertrophic growth in the absence of satellite cells following overload (McCarthy et al., 2017), supporting our finding that satellite cell expansion and hypertrophy are not necessarily dependent on each other.

Although HIIT did not induce a change in fiber size in our model, it did increase the proportion of oxidative fibers in wild-type mice. These findings corroborate previous work which showed a similar fiber type switch following lifelong physical activity in mice (Englund et al., 2020). The fiber type switch observed in the same study also occurred in satellite cell depleted mice, indicating that this metabolic adaption to exercise does not depend on satellite cells (Englund et al., 2020). Perhaps then, the increase in satellite cell number in wild-type mice following HIIT in our model is uncoupled to the metabolic changes within the muscle fibers. The prevention of fiber type switch after HIIT by the *klotho* transgene mirrors Klotho's effects on canonical Wnt signaling. However, whether these two processes are related is unknown.

In conclusion, our study demonstrates that HIIT induces satellite cell proliferation and activation, and that the *klotho* transgene attenuates these effects through the reduction of canonical Wnt signaling. Although the *klotho* transgene reduces early stages of myogenesis at the time point we conducted our study, increased markers of later stages of myogenesis indicate that Klotho may accelerate this process. These findings support previous study showing that Klotho can modulate myogenesis (Welc et al., 2019). Our study was conducted in 6-month mice, however investigations into HIIT in combination with the *klotho* transgene in aged mice could further elucidate the beneficial effects of Klotho. We also demonstrate interactions between

Klotho and canonical Wnt signaling. However further research into this pathway could uncover specific Wnt and target proteins that are impacted by Klotho.

A

High Intensity Interval Training (HIIT) ↓ 4 mo. — Sacrifice ↓ 6 mo.

Week	W0	W1	W2	W3	W4	W5	W6	W7	W8
Treadmill Incline (°)	0	10	15	20					
Treadmill Speed (m/min)	8	15-16				15-17	15-18	15-19	15-20

B

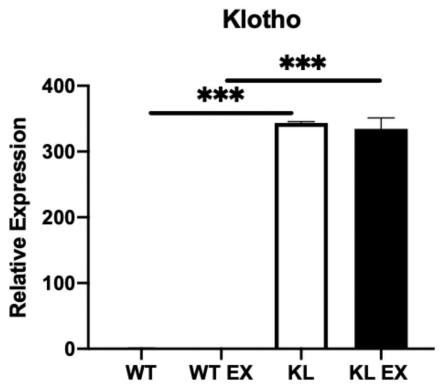

Figure 1. HIIT does not affect *klotho* expression in wild-type or *klotho* transgenic mice. **A)** Eight- week high intensity interval training protocol. **B)** Relative *klotho* gene expression in the tibialis anterior of 6-month wild-type and *klotho* transgenic mice with and without HIIT training (*** indicates $p < .001$). Data are presented as mean ± sem. P values are based on 2 -way ANOVA. WT: wild-type mice; KL: *klotho* transgenic mice; EX: exercise intervention.

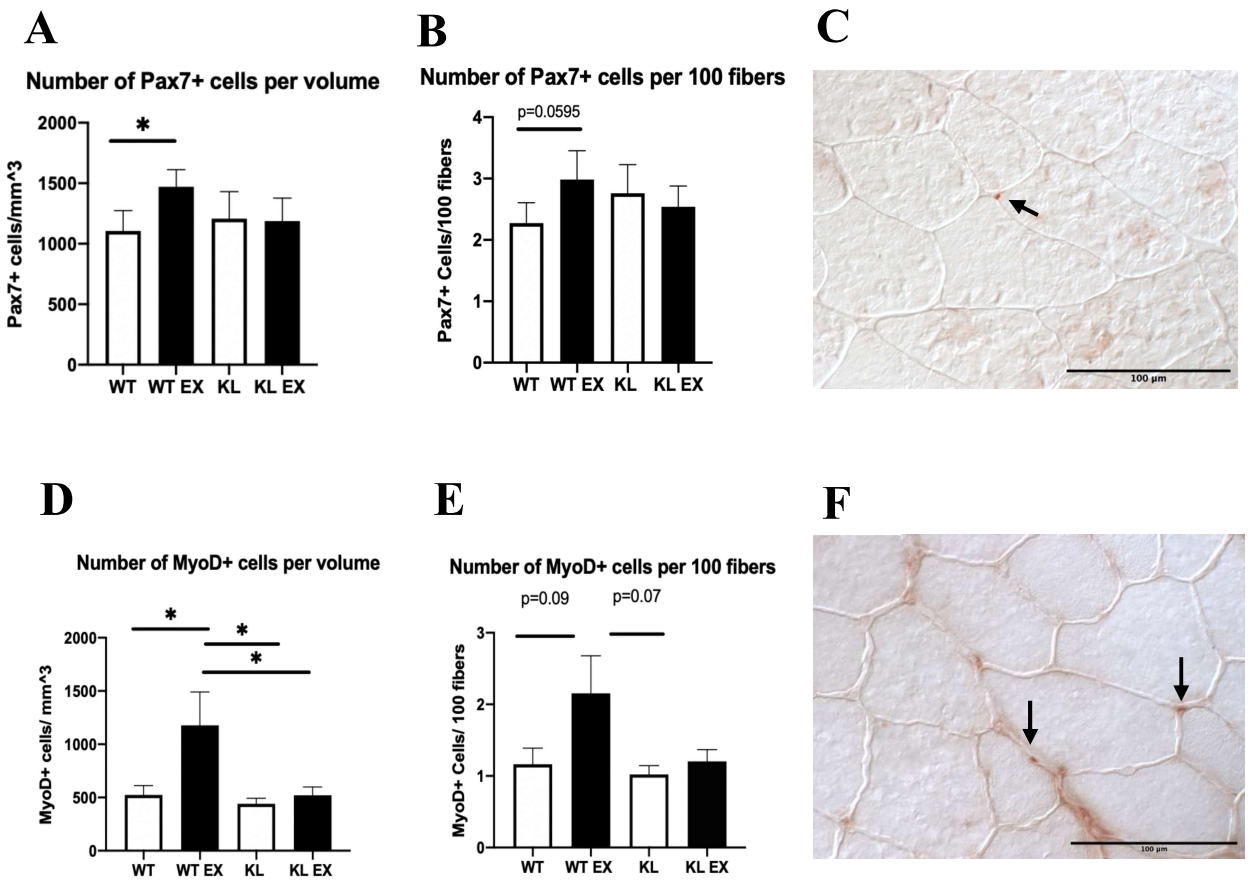

Figure 2. *Klotho* transgene expression attenuates the increase in numbers of total satellite cells and activated satellite cells caused by HIIT. **A-B)** Satellite cell numbers increased following HIIT exercise in wild-type mice and was attenuated by *klotho* transgene expression. Satellite cell numbers were quantified as number of cells per section volume **(A)** and per 100 fibers **(B)** (* indicates $p < 0.05$) **C)** Representative image of mouse tibialis anterior muscle showing location of (Pax7+) satellite cell. **D-E)** Numbers of activated satellite cells increased following HIIT in wild-type but not *klotho* transgenic mice. Activated satellite cell numbers were quantified as number of cells per section volume **(D)** and per 100 fibers **(E). F)** Representative image of mouse tibialis anterior muscle showing location of activated (MyoD+) satellite cells. Arrows indicate Pax7+ cells **(C)** and MyoD+ cells **(F).** Data are presented as mean ± sem. P values are based on 2 -way ANOVA. Scale bar = 100 µm

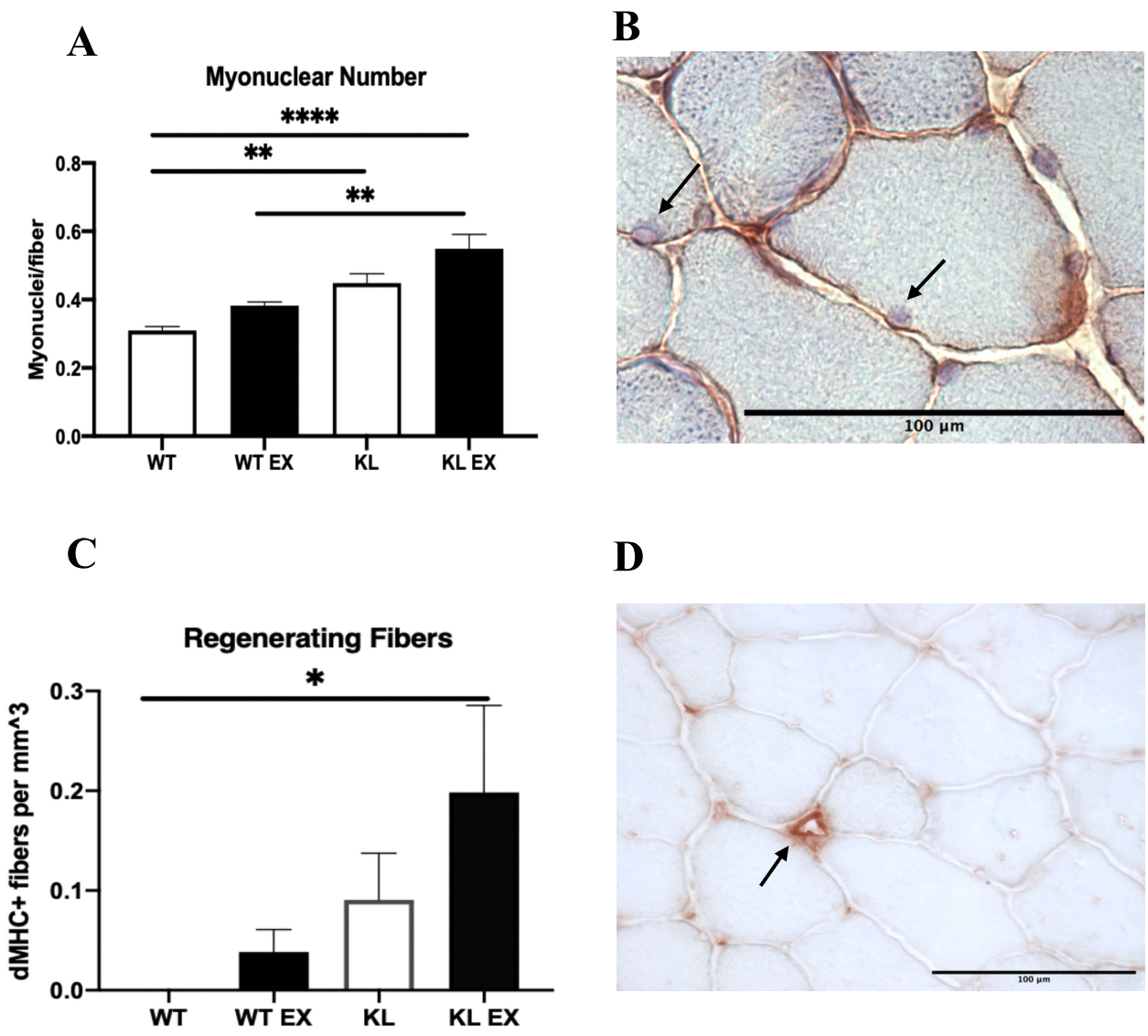

Figure 3. *Klotho* transgene expression in mice experiencing HIIT increases numbers of myonuclei and the number of dMHC+ fibers. **A)** Myonuclear number in the tibialis anterior muscles of 6-month wild-type and *klotho* transgenic mice with and without exercise (** indicates $p < 0.01$, *** *indicates $p < 0.0001$). **B)** Representative images of tibialis anterior muscle showing myonuclei location. Arrows indicate myonuclei **C)** Numbers of dMHC+ fibers in the tibialis anterior muscle of 6-month wild-type and *klotho* transgenic mice with and without exercise (* indicates $P < 0.05$). **D)** Representative image of mouse tibialis anterior muscle demonstrating a dMHC+ fiber with positive dMHC staining. Arrows indicate dMHC positive fibers. Data are presented as mean ± sem. P values are based on 2 -way ANOVA. Scale bar = 100 µm

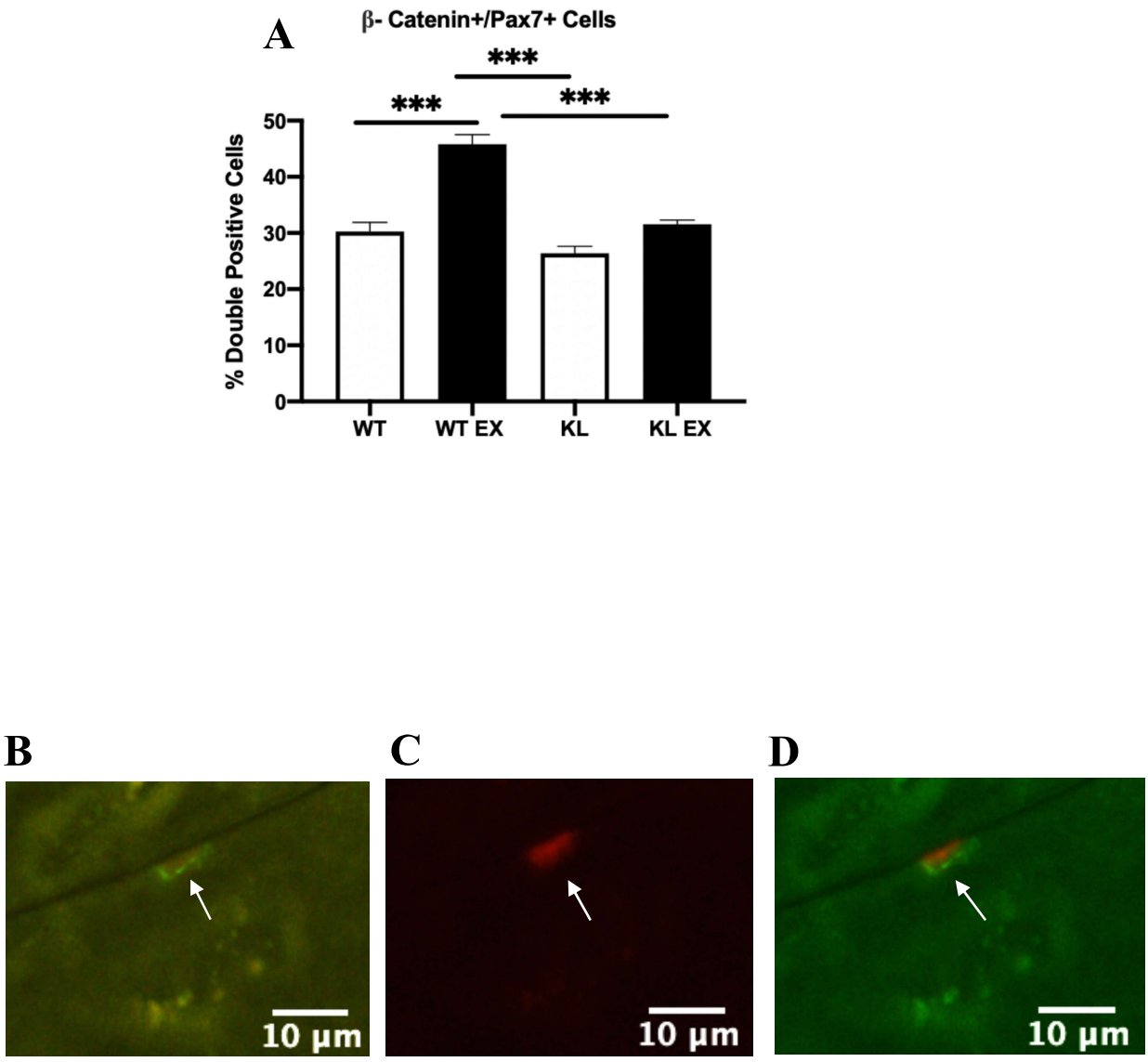

Figure 4. *Klotho* transgene expression prevents activation of the canonical Wnt pathway that results from HIIT. **A)** Percent of β-catenin+ satellite cells in the tibialis anterior muscle of 6-month mice with and without exercise (*** indicates P <0.001). **B-C)** Representative images of a satellite cell with β-catenin staining **(B)** that is Pax7+ **(C)**. **D)** Representative merged image of a satellite cell exhibiting Pax7 and β-catenin co-labeling. Data are presented as mean ± sem. P values are based on 2 -way ANOVA. Scale bar = 10 µm

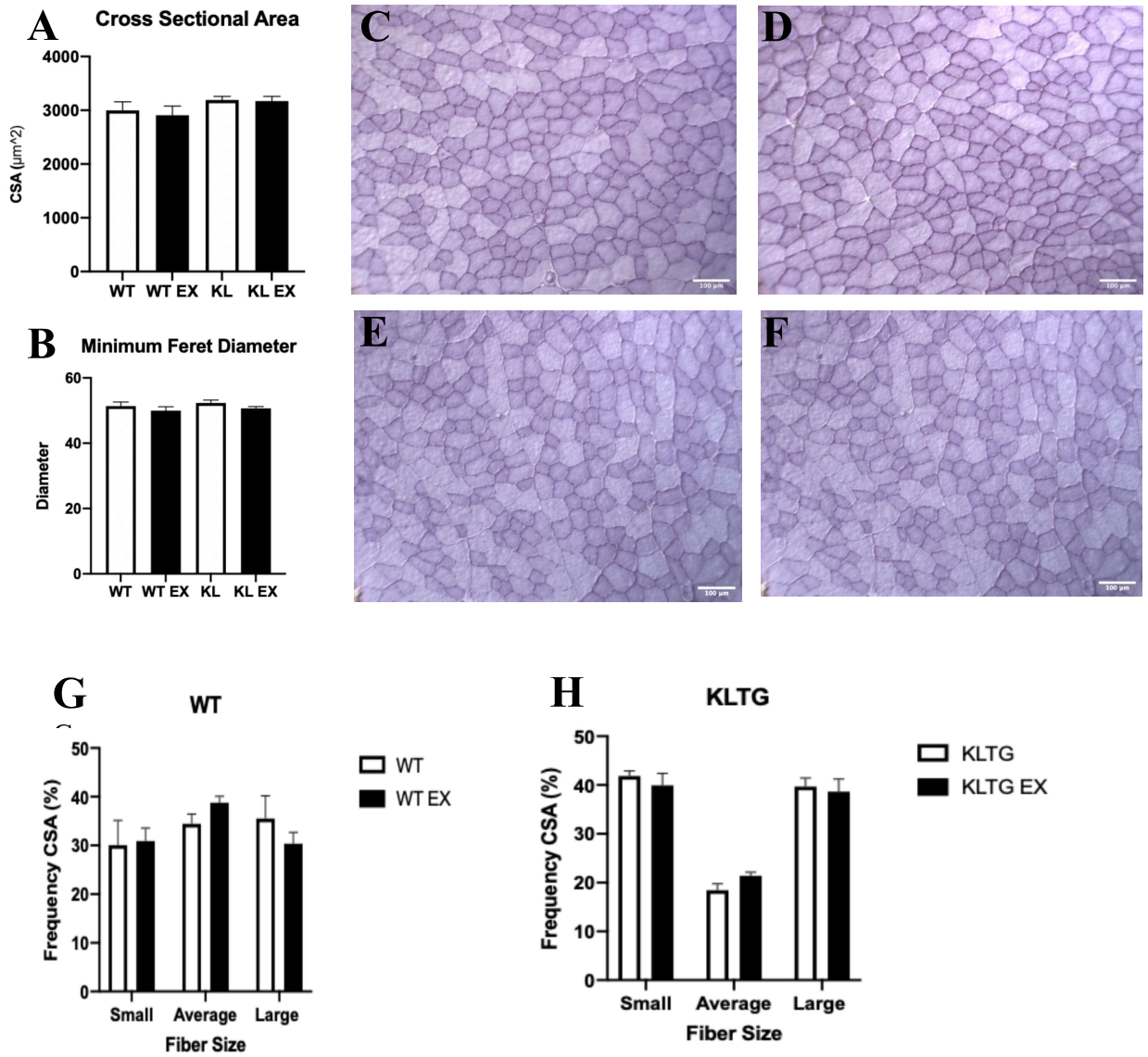

Figure 5. *Klotho* transgene expression increases the proportion of small diameter fibers in non-exercised and exercised muscles. **A)** Average cross-sectional area of fibers from wild-type and *klotho* transgenic mouse tibialis anterior with and without exercise. **B)** Average minimum ferret diameter of fibers from wild-type and *klotho* transgenic mouse tibialis anterior with and without exercise. **C-F)** Representative images of mouse tibialis anterior muscle cross section stained with hematoxylin, demonstrating no change in average fiber area or diameter between wild-type **(C)**, wild-type with exercise **(D)**, *klotho* transgenic **(E)** and *klotho* transgenic with exercise **(F)**. **G)** Frequency of wild-type average fiber sizes falling into small, average, and large fibers as determined by statistical analysis. Small fibers are fibers less than three standard deviations above the mean, and large fibers are more than three standard deviations above the mean. **H)** Frequency of *klotho* transgenic average fiber sizes falling into small, average, and large fibers as determined by statistical analysis. Small fibers are fibers less than three standard deviations above the mean, and large fibers are more than three standard deviations above the mean. Data are presented as mean ± sem. Scale bar = 100 μm

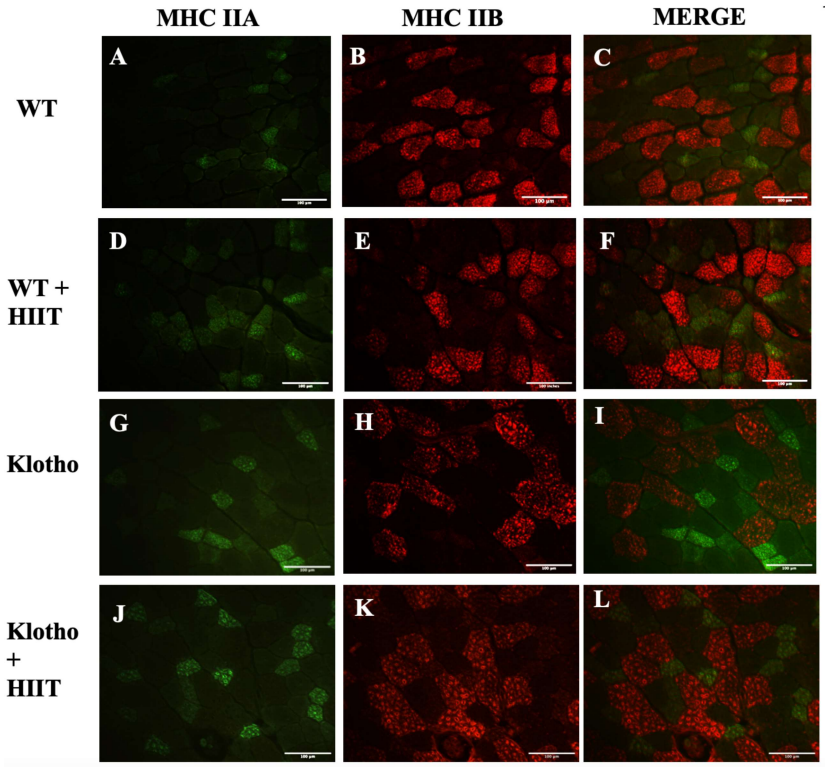

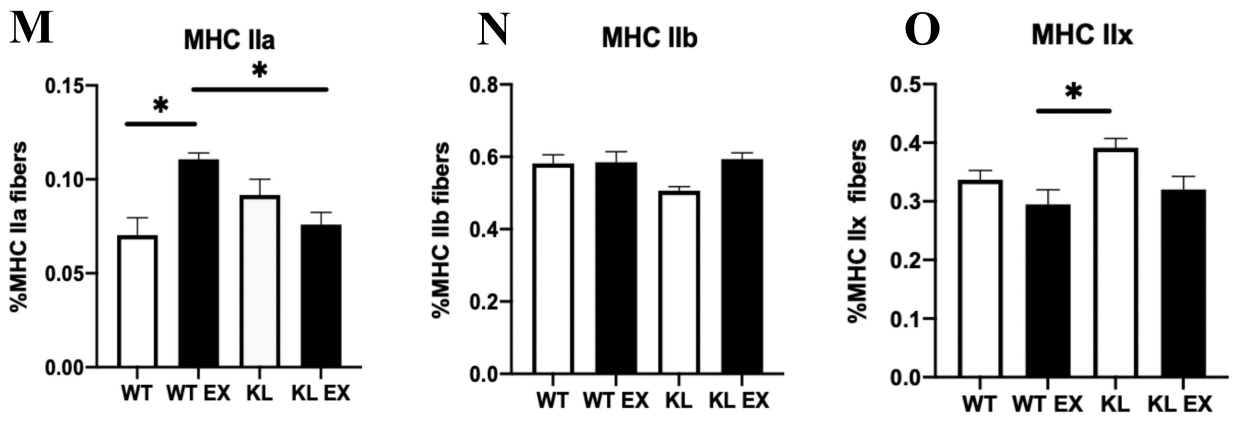

Figure 6. HIIT increases the proportion of MHC IIa fibers in wild-type but not *klotho* transgenic muscles. **A-L)** Representative images of fiber type distribution in the tibialis anterior muscle of 6-month wild-type and *klotho* transgenic mice with and without exercise. Numbers of MHC IIa fibers **(A,D,E,K)** were added to numbers of MHC IIb fibers **(B,E,H,K)** and subtracted from the total fiber number to determine number of type IIx fibers. **M)** Percent MHC IIa fibers of total fiber number in tibialis anterior muscle (* indicates $p < 0.05$) **N)** Percent MHC IIb fibers of total fiber number in tibialis anterior muscle **O)** Percent MHC IIx fibers of total fiber number in tibialis anterior muscle (* indicates $p < 0.05$). Data are presented as mean ± sem. P values are based on 2 -way ANOVA. Scale bar = 100 μm

References

1. Ahrens HE, Huettemeister J, Schmidt M, Kaether C, Von Maltzahn J (2018). Klotho expression is a prerequisite for proper muscle stem cell function and regeneration of skeletal muscle. *Skeletal Muscle* **8,** 20.
2. Bamman M, Roberts B, Adams G (2018). Molecular regulation of exercise-induced muscle fiber hypertrophy. *Cold Spring Harbor Perspectives in Medicine*, **33 (1),** 26-38.
3. Brooks M, Hajira A, Mohamed J, Alway S (1985). Voluntary wheel running increases satellite cell abundance and improves recovery from disuse in gastrocnemius muscles from mice. *Journal of Applied Physiology*, **124(6),** 1616-1628.
4. Chargé SBP & Rudnicki MA (2004). Cellular and molecular regulation of muscle regeneration. *Physiological Reviews* **84,** 209–238.
5. Dhawan J & Rando TA (2005). Stem cells in postnatal myogenesis: molecular mechanisms of satellite cell quiescence, activation and replenishment. *Trends in Cell Biology* **15,** 666–673.
6. Egner I, Bruusgaard J, Gunderson K (2016). Satellite cell depletion prevents fiber hypertrophy in skeletal muscle. *Development* **143(16)**, 2898-2906.
7. Englund D, Murach K, Dungan C, Figueiredo V, Vechetti I, Dupont-Versteegden E, McCarthy J, Peterson C (2020). Depletion of resident muscle stem cells negatively impacts running volume, physical function and muscle fiber hypertrophy in response to lifelong physical activity. *American Journal of Physiology*, **318**, C1178-C1188.

8. Fujimaki S, Hidaka R, Asashima M, Takemasa T & Kuwabara T (2014). Wnt protein-mediated satellite cell conversion in adult and aged mice following voluntary wheel running. *The Journal of Biological Chemistry,* **289***,* 7399-7411.
9. Fukimaki S, Wakabayashi T, Asashima M, Takemasa T, Tomoko K (2016). Treadmill running induces satellite cell activation in diabetic mice. *Biochemistry and Biophysics Reports*, **8**, 6-13.
10. Fujimaki S, Machida M, Wakabayashi T, Asashima M, Takemasa T, Kuwabara T (2016). Functional overload enhances satellite cell properties in skeletal muscle. *Stem Cells International*, **2016**, 7619418.
11. Goh Q, Song T, Petrany MJ, Cramer AAW, Sun C, Sadayappan S, Lee S & Millay D (2019). Myonuclear accretion is a determinant of exercise-induced remodeling in skeletal muscle. *eLife,* **8***,* 1-19.
12. McCarthy J, Mula J, Miyazaki M, Erfani R, Garrison K, Farooqui B, Srikeuea R, Lawson B, Grimes B, Keller C, Zant G, Campbell K, Esser K, Dupont-Versteegden E, Peterson C (2011). Effective fiber hypertrophy in satellite cell depleted skeletal muscle. *Development* **138(17)**, 3657-66.
13. McCarthy J, Dupont-Versteegden E, Fry C, Murach K, Peterson C (2017). Methodological issues limit interpretation of negative effects of satellite cell depletion on adult muscle hypertrophy. *Development* **144(8)**, 1363-1365.
14. Tatsumi R, Sheehan S.M, Iwasaki H, Hattori A, Allen R.E (2001). Mechanical stretch induces activation of skeletal muscle satellite cells in vitro. *Experimental Cell Research* **267 (1),** 107-114.

15. Tidball JG (2017). Regulation of muscle growth and regeneration by the immune system. *Nature Reviews Immunology* **17,** 165–178.

16. Wackerhage H, Schoenfeld B, Hamilton D, Lehti M, Hulmi J (2019). Stimuli and sensors that initiate skeletal muscle hypertrophy following resistance exercise. *Journal of Applied Physiology* **126**, 30-43.

17. Wehling-Henricks M, Li Z, Lindsey C, Wang Y, Welc SS, Ramos JN, Khanlou N, Kuro-O M & Tidball JG (2016). Klotho gene silencing promotes pathology in the mdx mouse model of Duchenne muscular dystrophy. *Human Molecular Genetics* **25,** 2465–2482.

18. Wehling-Henricks M, Welc S, Samengo G, Rinaldi C, Lindsey C, Wang Y, Lee J, Kuro-O M, Tidball J. G. (2018). Macrophages escape Klotho gene silencing in the *mdx* mouse model of Duchenne muscular dystrophy and promote muscle growth and increase satellite cell numbers through a Klotho-mediated pathway. *Human Molecular Genetics*, **27**, 14–29.

19. White RB, Biérinx A-S, Gnocchi VF & Zammit PS (2010). Dynamics of muscle fibre growth during postnatal mouse development. *BMC Developmental Biology* **10,** 21.

20. Lepper C, Partridge TA & Fan C-M (2011). An absolute requirement for Pax7-positive satellite cells in acute injury-induced skeletal muscle regeneration. *Development* **138,** 3639–3646.

21. Shefer G, Rauner G, Stuelsatz P, Benayahu D, Yablonka-Reuveni Z (2013). Moderate-intensity treadmill running promotes expansion of the satellite cell pool in young and old mice. *The FASEB Journal*, **280(17),** 4063-4073.